J Mater Sci (2012) 47:2033–2039
DOI 10.1007/s10853-011-6003-9

Structure and magnetic properties of soft organic ZnAl-LDH/polyimide electromagnetic shielding composites

Fengzhu Lv · Yueying Wu · Yihe Zhang · Jiwu Shang · Paul K. Chu

Received: 3 July 2011 / Accepted: 27 September 2011 / Published online: 12 October 2011

Abstract The imidization mechanism, structure, and magnetic properties of organic modified Zinc-aluminum layered double hydroxides/polyimide composites are investigated. During imidization, organic modified Zinc-aluminum layered double hydroxides lose the hydroxyl group and sodium dodecyl sulfate modifier decomposes partly resulting in a loose contact between PI and oxidized Zinc-aluminum layered double hydroxides. The thermal properties of composites are slightly decreased with increasing organic modified Zinc-aluminum layered double hydroxides but the wettability varies oppositely. Comparing to organic modified Zinc-aluminum layered double hydroxides, the saturated magnetization of heated organic modified Zinc-aluminum layered double hydroxides is enhanced slightly due to structural improvement in Fe_3O_4 crystalline domain. Therefore, the magnetic properties are not affected by imidization procedure. The soft magnetic composites have large potential in electromagnetic shielding.

Abbreviations

LDHs	Layered double hydroxides
PI	Polyimide
SDS	Sodium dodecyl sulfate
PMDA	Pyromellitic anhydride
ODA	4,4′-Oxydianiline
OZnAl-LDH	Organic magnetic ZnAl-LDH
DMAc	*N,N*-dimethylacetamide
PAA	Polyamic acid

F. Lv (✉) · Y. Wu · Y. Zhang (✉) · J. Shang
State Key Laboratory of Geological Processes & Mineral Resources, National Laboratory of Mineral Materials, School of Materials Science and Technology, China University of Geosciences (Beijing), Beijing 100083, China
e-mail: lfz619@cugb.edu.cn

Y. Zhang
e-mail: zyh@cugb.edu.cn

P. K. Chu
Department of Physics & Materials Science, City University of Hong Kong, Tat Chee Avenue, Kowloon, Hong Kong, China

Introduction

Layered double hydroxides (LDHs) constitute an important class of ionic lamellar solids originated from the isomorphous substitution of divalent cations, such as Mg^{2+}, by trivalent ones, such as Al^{3+}, in a planar brucite-like structure [1, 2], due to potential applications in ion exchange, catalysis, absorption, and antacids [3–9]. LDHs are also used as fillers in nanocomposite synthesis [10–15], because they not only improve the mechanical properties, but also serve as 2D construction blocks with a large aspect ratio. Furthermore, LDHs have specific advantages not matched by nanoclays made of layered silicates. In clay-polymer nanocomposites, the enforcing efficiency depends on the degree of exfoliation in the polymer matrix. A nanocomposite with fully exfoliated LDHs contains more exfoliated layers than a layered silicate-polymer nanocomposite because each layer of the LDHs consists of a single octahedral sheet of mixed metal hydroxide whereas clays are composed of multiple octahedral/tetrahedral sheets of metal oxide/hydroxide. Therefore, LDHs generally provide more efficient reinforcement at a lower filler concentration [15].

In LDH-containing nanocomposites, the nanosheets are not only used to improve the mechanical properties [16], but also serve as building blocks for the construction of the various functional nanocomposites or nanostructures. Guo [17] used LDH as filler in preparing polymeric materials stable under UV exposure. Leroux [18] prepared immiscible

polystyrene (PS) composites by direct incorporation of poly(AMPS) to the LDH phases to produce hybrid platelets used as an organo-modified 2D-type filler in PS. Enhanced dielectric properties were observed. Sasaki [19] reported the preparation of multilayered nanocomposites via layer-by-layer self-assembly of the exfoliated Co-Al LDH nanosheets and poly(sodium styrene4-sulfonate) and magnetic circular dichroism measurements revealed interesting magneto-optical response. In addition, LDHs were found to be suitable for flame retarding applications since the platelet surface was covered by hydroxyl groups and at a high temperature, the platelets turned into a ceramic barrier exhibiting self-extinguishing properties [20–22]. The functional properties of the composites depend on LDH exfoliation which can be promoted by modification with organic surfactants. Organic modification increases the interlayer distance (basal spacing) rendering the inorganic particles more hydrophobic and driving the polymer chains or chain segments into the interlayer space to improve the compatibility of the two phases [23]. Furthermore, since LDHs have a large aspect ratio, the nanosheet alignment is also critical. Linear fillers such as carbon nanotubes, carbon fibers, some magnetic particles and 2D nanosheets such as plate-like Fe_2O_3, graphene have been aligned in polymer matrices [24–28], the use of a magnetic field for this purpose has seldom been reported.

In this article, we prepare magnetic ZnAl-LDH with embedded Fe_3O_4 in the sheet and incorporated it in the polyimide (PI) matrix after modification by Sodium dodecyl sulfate (SDS). An external magnetic field is applied before imidization at room temperature to study the alignment of the magnetic LDH for the purpose of electromagnetic shielding. In this study, the effects of imidization on the structure and magnetic properties are studied.

Experimental

Materials

SDS was purchased from Xilong Chemical Corporation. Pyromellitic anhydride (PMDA) was obtained from Tianjin Tian yuan Electronic Material Company Limited and 4,4′-Oxydianiline (ODA) was bought from Japan Mitsubishi Chemical Corporation (MCC) and used without purification. All other chemicals and reagents were purchased from Beijing Chemical Reagent Factory. They were analytical grade and used without further purification.

Synthesis of magnetic nanoparticles

The magnetic nanoparticle was synthesized by co-precipitation [29]. The pH of the $FeCl_3{\cdot}6H_2O/FeSO_4{\cdot}7H_2O$ solution with a molar ratio of Fe(III)/Fe(II) = 1.8/1 was maintained at 10–11 by the addition of $NH_3{\cdot}H_2O$ under stirring and supersonic conditions at 65 °C. The mixture was maintained at this temperature for another 1 h. The precipitates were separated by a permanent magnet after aging for 1 h, washed thoroughly with deionized water and acetone, and then used directly.

Synthesis of magnetic ZnAl-LDH

The magnetic ZnAl-LDH precursor was synthesized by co-precipitation [30]. Two-hundred milliliter of an aqueous solution containing $Zn(NO_3)_2{\cdot}6H_2O$ (0.10 mol) and $Al(NO_3)_2{\cdot}9H_2O$ (0.05 mol) and 200 mL of an aqueous solution containing NaOH (0.33 mol) and Na_2CO_3 (0.10 mol) were added to a solution containing a certain amount of magnetic nanoparticles (Zn/Fe molar ratio = 17.86) under vigorous magnetic stirring at 65 °C. The mixture was aged at this temperature for 8 h (pH 10). The resultant suspension was filtered, washed four times by deionized water, and dried at 70 °C overnight.

Preparation of organic magnetic ZnAl-LDH

The organic magnetic ZnAl-LDH (OZnAl-LDH) was prepared by spontaneous self-assembly [26]. Seventy-five milliliter of the solution containing 0.02 mol $Zn(NO_3)_2{\cdot}6H_2O$ and 0.01 mol $Al(NO_3)_3{\cdot}9H_2O$ and 75 mL of the SDS solution (3.0 g) were added to a solution containing a certain amount of Fe_3O_4 at a pH of 10. The mixture was aged at 65 °C for 8 h. The resulting precipitate was filtered, washed by deionized water, and dried at 70 °C.

Preparation of magnetic OZnAl-LDH/PI nanocomposites

The OZnAl-LDH powders and 2.0024 g (0.0100 mol) of ODA were dispersed in *N,N*-dimethylacetamide (DMAc) ultrasonically for 3 h to obtain suspensions with different concentration of OZnAl-LDH. Then the suspension was put in a flask, 2.2139 g (0.0102 mol) of PMDA was added slowly under mechanical stirring. After the mixtures were stirred in an ice bath for 6 h, a viscous OZnAl-LDH/polyamic acid (PAA) solution was obtained. The viscous solutions were cast on clean glass plates and then a super magnet about 0.6 T was positioned parallel to the film to orient the magnetic OZnAl-LDH sheets. After drying in vacuum at 60 °C for 3 h under the external magnetic field, imidization was performed in a convection oven using the following thermal schedules: 80, 100, 130 and 170 °C for 30 min each and then 200, 250 and 300 °C for 1 h each to obtain the transparent OZnAl-LDH/PI films. The OZnAl-LDH contents in the composites relative to PI (ODA + PMDA) were 0, 0.5, 1, 3, 5, 7, 9 and 15 vol%.

Characterization and measurements

The X-ray diffraction patterns were recorded on a Rigaku D/Max-rA rotating anode X-ray diffractometer equipped with a Cu K_α tube and a Ni filter ($\lambda = 0.1542$ nm). Thermal gravimetric analyses (TGA) were performed on Perkin-Elmer TGA 7 with a heating rate of 20°/min ranging from 25° to 800°. The surface hydrophobicity of the films has been studied by contact angle measurements via the hanging drop method. The contact angle value is the average of the data obtained through measurement of one sample at three different positions by a JC2000D measurement meter at ambient temperature. The transmission electron microscopy (TEM) images were obtained on a FEI Tecnai G20 transmission electron microanalyser at an accelerating voltage of 200 kV. The fresh surface of the composite film was formed by an ion beam cutting parallel to the film surface at room temperature. The magnetic hysteresis loops were recorded on a PPMS-9T Vibrating sample magnetometer.

Results and discussion

Recently study on the alignment of magnetic OZnAl-LDH in PI matrix was carried out in our lab. The XRD patterns of the magnetic ZnAl-LDH, OZnAl-LDH, oxidized OZnAl-LDH, pure PI, OZnAl-LDH/PI with 7 vol% OZnAl-LDH prepared under the magnetic field parallel to the plane of film, as well as without the magnetic field are shown in Fig. 1a–f, respectively. These diffraction patterns reveal the structural changes in the samples. The magnetic ZnAl-LDH and OZnAl-LDH have well-crystallized lamellar structure with 3R rhombic symmetry shown in Fig. 1a, b [31]. To verify the structural change of OZnAl-LDH in the OZnAl-LDH/PI, the OZnAl-LDH powders are heated similarly as the procedure of imidization and the XRD pattern (Fig. 1c) does not show the characteristic diffraction peaks of ZnAl-LDH. Therefore, the disappearance of the characteristic peaks of LDH in the composites (Fig. 1e, f) may derive from the complete exploiting or the structure change.

Figure 2 displays the TGA curves of ZnAl-LDH, OZnAl-LDH, pure PI and OZnAl-LDH/PI nanocomposites prepared with various OZnAl-LDH contents under the magnetic field parallel to the plane of film. Thermal analysis of ZnAl-LDH shows a mass loss in the range of 100–190 °C due to the removal of interlayer water molecules which has close interaction with the hydroxide layer and/or interlayer anion via hydrogen bonding [23, 24]. The rapid mass loss at the higher temperature range (190–320 °C) stems from dehydroxylation of the LDH basal layers and it further decreases at 480–610 °C as a result of the loss of interlayer carbonate. The mass loss of OZnAl-LDH can be divided into three stages. Between 25 and 170 °C, the weight loss stems from loss of absorbed water. Between 170 and 410 °C, collapse of the crystalline structure results in dehydroxylation of the host layers in the OZnAl-LDH and decomposition of the SDS alkyl chain, whereas decomposition of the sulfuric group is responsible for the behavior observed between 580 and 800 °C. Our results show that the dehydroxylation temperature of the host layers in SDS-LDH is lower than that in LDH as consistent with previous reports on MgAl-LDH intercalated by SDS via regeneration [16, 23]. As can been seen in Fig. 2, the weight of the SDS-LDH residue (64%) is greater than that of LDH (56%) and it can be attributed to the

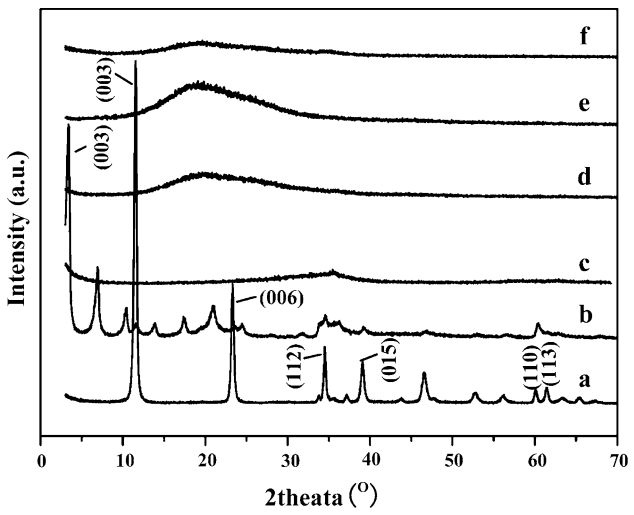

Fig. 1 XRD patterns of *a* magnetic ZnAl-LDH, *b* magnetic OZnAl-LDH, *c* oxidized OZnAl-LDH, *d* pure PI, *e* OZnAl-LDH/PI with 7 vol% OZnAl-LDH prepared under the magnetic field parallel to the plane of film, as well as without the magnetic field (*f*)

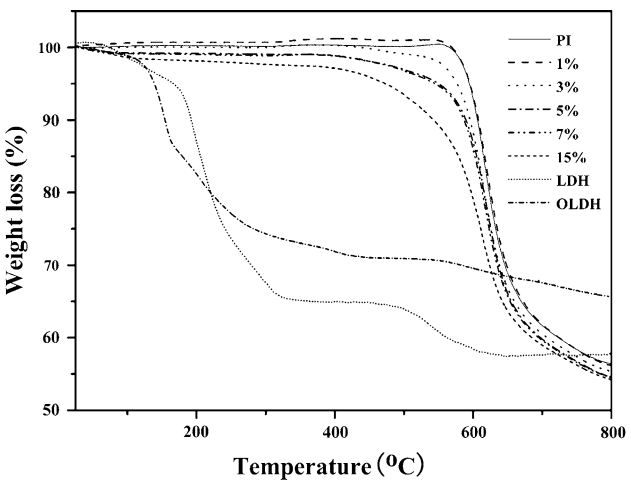

Fig. 2 TGA curves of ZnAl-LDH, OZnAl-LDH, PI and OZnAl-LDH/PI nanocomposites prepared with various LDH contents under the magnetic field parallel to the plane of film

lower adsorption of water and incomplete decomposition of sulfuric group [32]. The temperature of dehydroxylation in the host layer and decomposition of alkyl chain of SDS is in the range of the imidization temperature. Therefore, it can be inferred that during the imidization of OZnAl-LDH/PI composites, the SDS may partly decompose and the residues influence the thermal properties of the composites.

The weight loss data of the composites summarized in Table 1 indicate obvious mass loss is tested out as the OZnAl-LDH content is larger than 5 vol% when the temperature is below 100 °C although no reaction could take place. These results illuminate some water molecules have been adsorbed on the surface of the composites due to the relatively hydrophilic OZnAl-LDH loading. To corroborate the weight loss results, contact angle measurement are conducted. The contact angle variation is a direct evidence of hydrophilic or hydrophobic change of a surface [33]. Larger contact angle means lower hydrophilic property of the measured surface. The contact angles of composite films with 0, 1, 3, 5, 7 and 15 vol% OZnAl-LDH are 78.5, 76.3, 76.0, 75.0, 69.0 and 61.5°, respectively (Fig. 3), demonstrating that the hydrophilic property increases with OZnAl-LDH concentration. The contact angle variances of above composite films are 0.75, 0.08, 0.25, 0.08, 0.25, 0.25, respectively.

At the temperature of dehydroxylation of OZnAl-LDH basal layers and decomposition of SDS (Fig. 2), the weight loss of the composites (summarized in Table 1) between 100 and 350 °C is not serious. This indicates that in the process of imidization, dehydroxylation of the OZnAl-LDH basal layers and decomposition of SDS are almost completed. Further decrease at the higher temperature range (350–450 °C) arises from the decomposition of the polymer matrix because of the relatively weak interaction between the PI and OZnAl-LDH. The temperature of 5% weight loss of the samples with 0, 1, 3, 5, 7, 15 vol% OZnAl-LDH is 594, 595, 576, 550, 545, 473 °C, respectively. Since 5% weight loss is an index of material resistance heat, the weight loss (which is the contribution of absorption water) below 100 °C could not be included in. After deduction the contribution of absorption water,

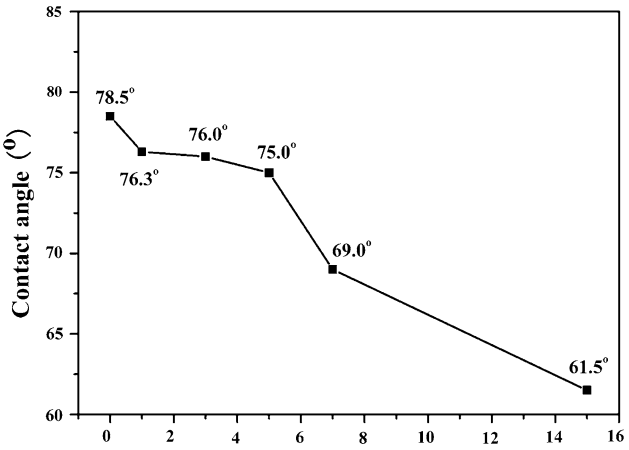

Fig. 3 The contact angles of the composite films with different content of OZnAl-LDH

the temperature of 5% weight loss changes to be 594, 595, 576, 559, 558, 499 °C, respectively. The reduction in thermal resistance with increasing OZnAl-LDH is ascribed to the decomposition of SDS and LDH along with imidization of PAA and the relatively loose stack between oxided OZnAl-LDH and PI. This trend is somewhat different from that observed from the MgAl-LDH and PI system [11]. This is because in the latter, the modifier is grafted onto the PI molecules and there are no small molecules in the process of imidization. Although the introduction of OZnAl-LDH decreases the thermal properties, the temperature of 5% weight loss is still larger than 550 °C when the amount of OZnAl-LDH is lower than 15%. Hence, good thermal resistance is still demonstrated.

Schematic representation of the OZnAl-LDH/PAA preparation and imidization is shown in Scheme 1. When PMDA is introduced into the system of OZnAl-LDH/ODA/DMAc, the anhydride groups of PMDA react with the amine functional groups of ODA and PAA is formed. The higher molecule weight of PAA enlarges the interlayer spacing and enforces exfoliation of ZnAl-LDH. The disordered nanolayers are well dispersed in the PAA matrix to form the OZnAl-LDH/PAA nanocomposites. While in the process of imidization, dehydroxidation of PAA, decomposition of

Table 1 Mass losses measured from the composites at different temperatures

Temperature range (°C)	Mass loss of the composites (%)					
	0[a]	1	3	5	7	15
25–100	0	0	0	0.7	0.9	1.4
100–180	0	0	0	0.1	0.1	0.4
180–220	0	0	0	0.1	0.1	0.2
220–350	0	0	0	0.1	0.1	0.5
350–450	0	0	0.2	0.8	0.8	1.7

[a] Samples with different LDH contents (vol%)

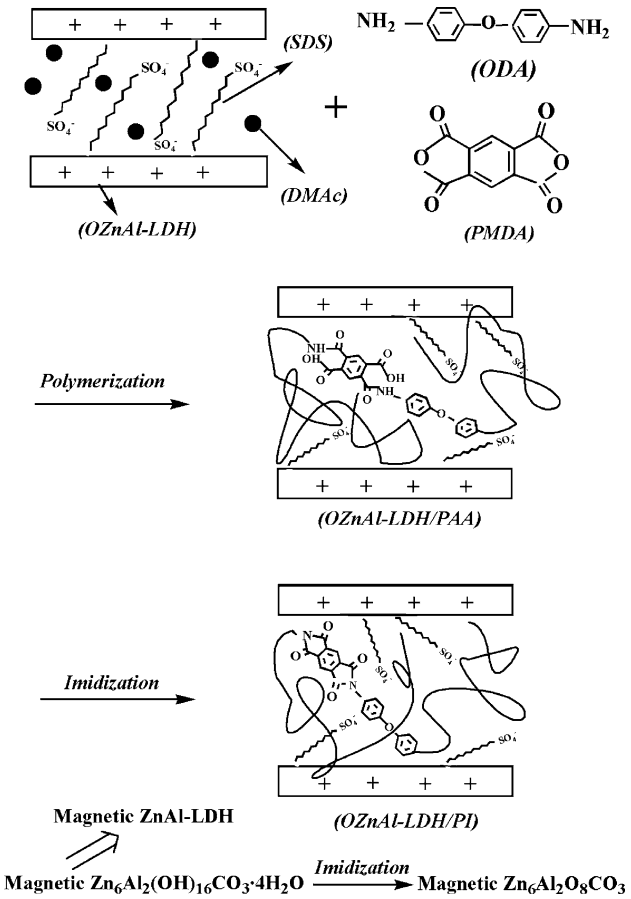

Scheme 1 Schematic representation of the OZnAl-LDH/PAA preparation and imidization

SDS, and dehydroxylation of LDH take place and LDH is converted into oxides. The reaction of ZnAl-LDH and the imidization of PAA can be expressed as the bottom equation:

$$\text{Magnetic } Zn_6Al_2(OH)_{16}CO_3 \cdot 4H_2O \xrightarrow{\text{Imidization}} \text{Magnetic } Zn_6Al_2O_8CO_3 \quad (1)$$

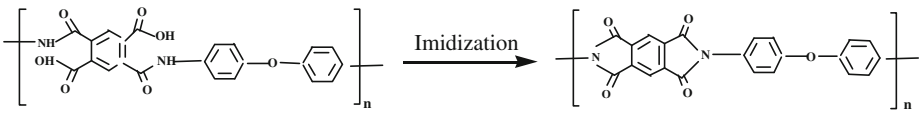

(2)

Figure 4 depicts the TEM photograph of the fresh face of the OZnAl-LDH/PI composite film with 7 vol% OZnAl-LDH prepared without the magnetic field. This fresh surface is formed after ion beam milling parallel to the film surface. The oxidized OZnAl-LDH well dispersed in the matrix resembles a single hexagonal sheet. This demonstrates that the lamellar structure is reserved during imidization.

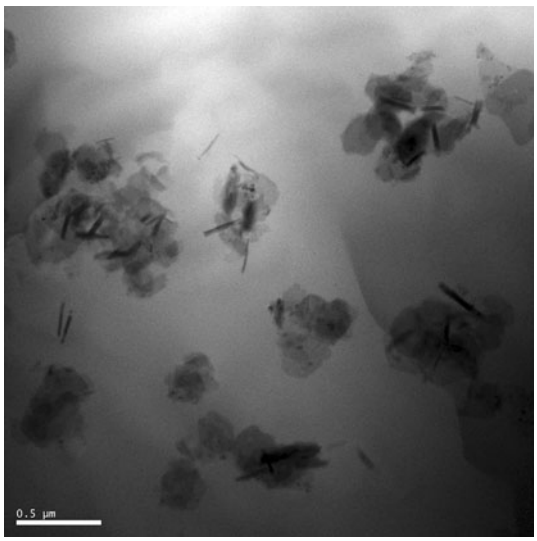

Fig. 4 TEM photograph of the internal structure of the magnetic OZnAl-LDH/PI with 7 vol% OZnAl-LDH

The magnetic properties of the OZnAl-LDH are determined. The suspension of magnetic OZnAl-LDH in water exhibits good response to the external magnetic field (Fig. 5b). When the magnetic field is withdrawn, the magnetic OZnAl-LDH disperses homogenously under ultrasonic or stirring (Fig. 5a) because of the low remanence and coercivity. Our results also demonstrate that every sheet of the as-prepared OZnAl-LDH contains magnetic particles and responds to an external magnet field. Figure 6 depicts the magnetization (M) versus magnetic field (H) curve of the magnetic OZnAl-LDH at room temperature. The OZnAl-LDH powders have obvious ferromagnetic characteristics. The hysteresis loop is closed and the saturation magnetization (M_s) of the OZnAl-LDH powders is up to 1.68 emu/g due to the small Fe content (Zn/Fe molar ratio = 17.86). The coercivity (H_c) and negligible remanence (M_r) are about 48 Oe and 0.04 emu/g, respectively. The relatively low H_c and M_r values signify that these micro-particles are not magnetized at zero applied field illustrating a typical paramagnetic behavior and that the single-domain magnetic nanoparticles are separated entirely. The remanence ratio, M_r/M_s, differentiates between the SD (single-domain) and non-SD particle behavior. According to Stoner and Wohlfarth [34], a remanence ratio of 0.5 results only from a random

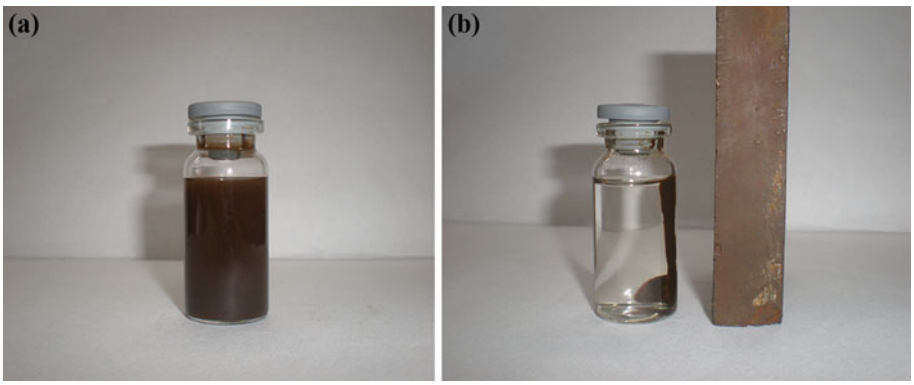

Fig. 5 The photos of magnetic OZnAl-LDH suspended in water **a** in the absence and **b** the presence of an external magnet

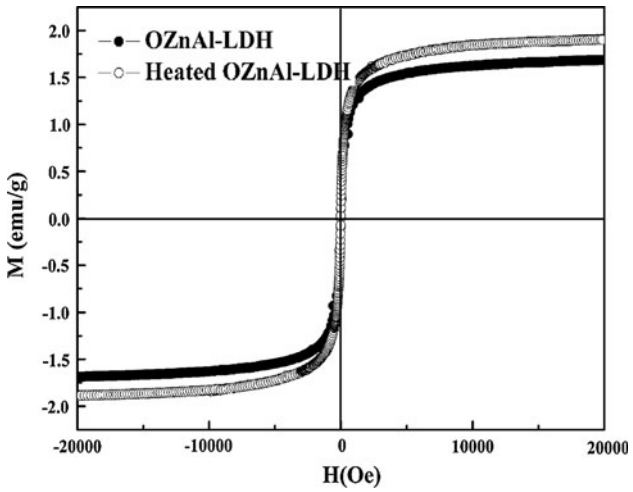

Fig. 6 Magnetic hysteresis loops of the magnetic OZnAl-LDH and the heated OZnAl-LDH which was treated in the same way as imidization of OZnAl-LDH/PAA

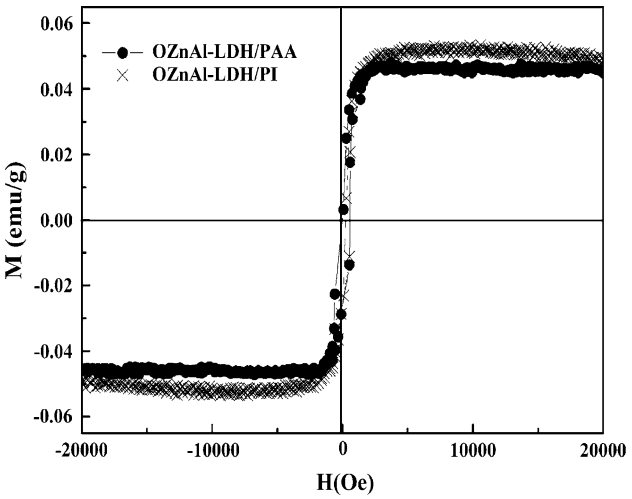

Fig. 7 Magnetic hysteresis loops of the OZnAl-LDH/PAA and OZnAl-LDH/PI nanocomposites with 7 vol% OZnAl-LDH prepared under the magnetic field parallel to the plane of films

distribution of non-interacting uniaxial particles whereas a remanence ratio of less than 0.1 is typically observed for the multi-domain case. The remanence ratio of our materials is 0.03 which indicates a uniform distribution of Fe_3O_4 in the OZnAl-LDH and formation of a uniform micro-domain.

The magnetic properties of materials depend on the temperature, and so the influence of imidization on the magnetic properties of the composites is evaluated. After heat treatment in the similar way as imidization of OZnAl-LDH/PAA, the M_s of the heated OZnAl-LDH increases to 1.90 emu/g. According to the literature, the solid phase reaction of Fe_3O_4 with ZnO takes place at about 1000 K to give $ZnFe_2O_4$ magnetic particles [35]. Meanwhile, oxidation of Fe_3O_4 is not dominant due to the protection effect of the SDS and polymer molecules during imidization. Therefore, the increase in saturation magnetization can be ascribed to the structural improvement in the Fe_3O_4 crystalline domain, although the subtle change cannot be revealed unequivocally by XRD due to its low content and small size. Figure 7 displays the magnetic hysteresis loops of the magnetic OZnAl-LDH/PAA and OZnAl-LDH/PI nanocomposites with 7 vol% OZnAl-LDH acquired at the room temperature under a magnetic field parallel to the plane of the sample. In general, the specific saturation magnetization (M_s) of soft magnetic polymeric composite microspheres at 300 K is lower than that of Fe_3O_4 nanoparticles. The M_s value is only about 0.05 for the OZnAl-LDH/PI nanocomposites prepared with a magnet field parallel to the surface and it is in agreement with previous results [36, 37]. The M_s value and the magnetic hysteresis loop style of OZnAl-LDH/PAA were almost the same as OZnAl-LDH/PI indicating that the magnetic property of the composites had not obvious change in the process of imidization and the magnetic property of the composites is independence of temperature.

Conclusions

Magnetic OZnAl-LDH/PI composite films were prepared by in situ polymerization. The influence of imidization procedure on the structure, thermal and magnetic properties

was discussed in detail. The results showed that in the imidization process of PAA, the LDH lost the hydroxy of the host layers and the SDS modifier decomposed partly, resulting in relatively loose contact between PI and oxidized LDH. The thermal property of the composites slightly decreased with increasing OZnAl-LDH but the wettability varies oppositely. The saturated magnetization of OZnAl-LDH was enhanced slightly due to the crystallity improvement in the Fe_3O_4 domain under the protection of SDS. However, the magnetic properties of OZnAl-LDH/PI composite films were not affected by the imidization procedure. The soft magnetic composite materials have the large potential applications in electromagnetic shielding.

Acknowledgements The study was financially supported by the Fundamental Research Funds for the Central Universities (2010ZY46), National Key Laboratory of Minerals (09B003), China, Key Project of Chinese Ministry of Education (107023), Special fund of Co-construction of Beijing Education Committee, and City University of Hong Kong Strategic Research Grant (SRG, 7008009).

References

1. Cavani F, Trifiro F, Vaccari A (1991) Catal Today 11:173
2. Naime Filho JF, Silvério F, dos Reis MJ, Valim JB (2008) J Mater Sci 43:6986. doi:10.1007/s10853-008-2952-z
3. Carpani I, Berrettoni M, Blaring B, Giorgetti M, Scavetta E, Tonelli D (2004) Solid State Ionics 168:167
4. Terry PA (2004) Chemosphere 57:541
5. Vaccari A (1999) Appl Clay Sci 14:161
6. Bouraada M, Belhalfaoui F, Ouali MS (2009) J Hazard Mater 163:463
7. Zhang LH, Li F, Evans DG, Duan X (2010) J Mater Sci 45:3741. doi:10.1007/s10853-010-4423-6
8. Nhlapo N, Motumi T, Landman E, Verryn SMC, Focke WW (2008) J Mater Sci 43:1033. doi:10.1007/s10853-007-2251-0
9. Moyo L, Nhlapo N, Focke WW (2008) J Mater Sci 43:6144. doi:10.1007/s10853-008-2935-0
10. Leroux F, Besse JP (2003) Chem Mater 13:3507
11. Hsueh HB, Chen CY (2003) Polymer 44:1151
12. Hsueh HB, Chen CY (2003) Polymer 44:5257
13. Chen B, Qu B (2003) Chem Mater 15:3208
14. Costa FR, Goad MA, Wagenknecht U, Heinrich G (2005) Polymer 46:4447
15. O'Leary S, O'Hare D, Seeley G (2002) Chem Commun 14:1506
16. Costa FR, Leuteritz A, Wagenknecht U, Jehnichen D, Häußler L, Heinrich G (2008) Appl Clay Sci 38:164
17. Guo S, Evans DG, Li D (2006) J Phys Chem Solids 67:1002
18. Leroux F, Illaik A, Stimpfling T, Troutier-Thuilliez AL, Fleutot S, Martinez H, Cellier J, Verney V (2010) J Mater Chem 20:9484
19. Liu ZP, Ma R, Osada M, Iyi N, Ebina Y, Takada K, Sasaki T (2006) J Am Chem Soc 128:4872
20. Zammarano M, Franceschi M, Bellayer S, Gilmanand JW, Meriani S (2005) Polymer 46:9314
21. Qiu L, Chen W, Qu B (2006) Polymer 47:922
22. Costa FR, Wagenknecht U, Heinrich G (2007) Polym Degrad Stab 92:1813
23. Costa FR, Leuteritz A, Wagenknecht U, Landwehr MA, Jehnichen D, Haeussler L, Heinrich G (2009) Appl Clay Sci 44:7
24. Kimura T, Ago H, Tobita M, Ohshima S, Kyotani M, Yumura M (2006) Adv Mater 14:1380
25. Tian Y, Park JG, Cheng Q, Liang Z, Zhang C, Wang B (2009) Nanotechnology 20:335601
26. Dyab AKF, Ozmen M, Ersoz M, Paunov VN (2009) J Mater Chem 19:3475
27. Liu S, Zhou J, Zhang L, Guan J, Wang (2006) J Macromol Rapid Commun 27:2084
28. Wang HQ, Zhang HY, Zhao WF, Zhang W, Chen GH (2008) Compos Sci Technol 68:238
29. Wang J, You J, Li ZS, Yang PP, Jing XY, Zhang ML (2008) Nanoscale Res Lett 3:338
30. Wang J, Liu Q, Zhang G, Li Z, Yang P, Jing X, Zhang M, Liu T, Jiang Z (2009) Solid State Sci 11:1597
31. Aisawa S, Kudo H, Hoshi T, Takahashi S, Hirahara H, Umetsu Y, Narita E (2004) J Solid State Chem 177:3987
32. Trujillano R, Holgado MJ, González JL, Rives V (2005) Solid State Sci 7:931
33. Balogh D, Tel-Vered R, Riskin M, Orbach R, Willner I (2011) ACS Nano 5:299
34. Iannotti V, Amoruso S, Ausanio G, Barone AC, Campana C, Hison C, Wang X (2003) J Appl Phys 93:7041
35. Su HC, Dai JY, Liao YF, Wu YH, Huang JCA, Lee CH (2010) Thin Solid Films 518:7275
36. Ramirez LP, Landfester K (2003) Macromol Chem Phys 204:22
37. Fan LH, Luo YL, Chen YS, Zhang CH, Wei QB (2009) J Nanopart Res 11:449